Optical constants of silica glass from extreme ultraviolet to far infrared at near room temperature

Rei Kitamura,[1] Laurent Pilon,[1,*] and Miroslaw Jonasz[2]

[1]Department of Mechanical and Aerospace Engineering, Henry Samueli School of Engineering and Applied Science, University of California, Los Angeles, Los Angeles, California 90095, USA

[2]MJC Optical Technology, 217 Cadillac Street, Beaconsfield, QC H9W 2W7, Canada

*Corresponding author: pilon@seas.ucla.edu

Received 30 July 2007; accepted 31 August 2007;
posted 25 September 2007 (Doc. ID 85883); published 19 November 2007

We thoroughly and critically review studies reporting the real (refractive index) and imaginary (absorption index) parts of the complex refractive index of silica glass over the spectral range from 30 nm to 1000 μm. The general features of the optical constants over the electromagnetic spectrum are relatively consistent throughout the literature. In particular, silica glass is effectively opaque for wavelengths shorter than 200 nm and larger than 3.5–4.0 μm. Strong absorption bands are observed (i) below 160 nm due to the interaction with electrons, absorption by impurities, and the presence of OH groups and point defects; (ii) at ~2.73–2.85, 3.5, and 4.3 μm also caused by OH groups; and (iii) at ~9–9.5, 12.5, and 21–23 μm due to Si—O—Si resonance modes of vibration. However, the actual values of the refractive and absorption indices can vary significantly due to the glass manufacturing process, crystallinity, wavelength, and temperature and to the presence of impurities, point defects, inclusions, and bubbles, as well as to the experimental uncertainties and approximations in the retrieval methods. Moreover, new formulas providing comprehensive approximations of the optical properties of silica glass are proposed between 7 and 50 μm. These formulas are consistent with experimental data and substantially extend the spectral range of 0.21–7 μm covered by existing formulas and can be used in various engineering applications. © 2007 Optical Society of America

OCIS codes: 160.6030, 160.4760, 290.3030, 160.4670, 050.5298, 110.5220.

1. Introduction

Silicon dioxide (SiO_2 or silica) has many forms including three main crystalline varieties: quartz, tridymite, and cristobalite [1,2]. Silica can also exist in noncrystalline form as silica glass or vitreous silica [1], also referred to as amorphous silica and glassy silica. There are four basic types of commercial silica glasses [3,4]: (1) Type I is obtained by the electric melting of natural quartz crystal in vacuum or in an inert gas at low pressure, (2) Type II is produced from quartz crystal powder by flame fusion, (3) Type III is synthetic and produced by the hydrolyzation of $SiCl_4$ when sprayed into an OH flame, and (4) Type IV is also synthetic and produced from $SiCl_4$ in a water vapor-free plasma flame.

0003-6935/07/338118-16$15.00/0
© 2007 Optical Society of America

Each type of silica glass has its own impurity level and optical properties. For example, Type I silica glasses tend to contain metallic impurities [3,4]. On the other hand, Types III and IV are much purer than Type I and feature greater ultraviolet (UV) transmission [3,4]. However, Type III silica glasses have, in general, higher water content, and infrared (IR) transmission is limited by strong water absorption peaks at wavelengths around 2.2 and 2.7 μm [3–5]. Type IV is similar to Type III but contains less water and thus has better IR transmission. Suppliers provide various product grades for different optical applications [3,4,6]. Trade names for Type I silica glass are Infrasil, IR-Vitreosil, Pursil, and GE 105, for example. On the other hand, KU, Herosil, Homosil, Vitrasil, and OG Vitreosil are Type II. Moreover, KU-1, KV, Suprasil I, Tetrasil, Spectrosil, and Corning 7940 are known as synthetic fused silica and classified as Type III. Finally, KI, Suprasil W, Spectrosil WF, and Corning 7943 are Type IV silica glass. The term "fused quartz" is usually used for Type I and "fused silica" is used for synthetic fused silica, i.e., Types III or IV. In practice, however, those terms are often used interchangeably.

Because of its favorable physical, chemical, and optical characteristics, silica glass has been used in numerous applications: (1) as laboratory glassware, (2) in optics, as lenses or beam splitters, (3) for lighting and IR heating, (4) in telecommunications, as fiber optics, (5) in micro- and optoelectronics, as a dielectric insulator, a waveguide, photonic crystal fibers, or projection masks for photolithography, and (6) in thermal protection systems, as fibrous thermal insulation. In all these applications, optical properties are essential to predict and optimize the optical and thermal radiation performances of this material. Silica fiber optics, for example, are used in the near-IR at ~1.31 and 1.55 μm due to their low optical attenuation and optical dispersion [7,8]. In lens designing, one often needs to fit and interpolate refractive index data that are reported or measured at discrete wavelengths over certain spectral regions [9,10]. On the other hand, astronomers and atmospheric scientists are interested in the optical properties of interstellar and atmospheric silica particles in the mid- and far-IR region of the spectrum [11–13].

The complex refractive index, m_λ, of silica glass at wavelength λ is defined as

$$m_\lambda = n_\lambda + ik_\lambda, \tag{1}$$

where n_λ is the refractive index and k_λ is the absorption index. The wavelength λ is related to other quantities such as frequency ν and wavenumber η according to

$$\lambda = \frac{c_\lambda}{\nu} = \frac{1}{\eta}, \tag{2}$$

where c_λ is the speed of light at wavelength λ in vacuum. Therefore, the refractive and absorption indices can also be expressed as functions of frequency and denoted by n_ν and k_ν or as functions of wavenumber and denoted by n_η and k_η.

The experimental data for the refractive and absorption indices vary in precision depending on the measurement techniques used and on the approximations made in retrieving the intrinsic optical properties. One should also keep in mind that these optical properties may be sensitive to the presence of impurities, crystallinity, point defects, inclusions, bubbles, wavelength, temperature, and the glass manufacturing process. In addition, when considering the literature it is often difficult to choose the set of experimental data or formula to use and to assess its validity. The objectives of this paper are (1) to critically review and compare the experimental data reported in the literature for the complex refractive index of silica glass and (2) to develop formulas that provide a comprehensive approximation of the measured data near room temperature. Given the wide range of engineering and scientific applications, the spectral range from 30 nm to 1000 μm is considered.

2. Experimental Methods

A. Refractive Index, n_λ

Various experimental techniques and procedures have been used to retrieve the real part of the complex refractive index n_λ. The most accurate is the minimum deviation angle method [14], which relies on measuring the minimum deviation angle $\theta_{\min}$ of an isosceles triangular prism made of the silica glass placed in air. This method is based on Snell's law [14], and the refractive index n_λ can be estimated by

$$n_\lambda = \frac{\sin\left(\dfrac{\theta_{\min} + \phi}{2}\right)}{\sin\left(\dfrac{\phi}{2}\right)} n_{\text{air}}, \tag{3}$$

where ϕ is an apex angle of the prism sample and n_{air} is the refractive index of air ($n_{\text{air}} = 1$). This method is often used to accurately measure the refractive index of highly transparent glass for which the absorption index k_λ, i.e., the imaginary part of the complex refractive index, is negligibly small.

Alternatively, the interferometric method is also used to measure n_λ. It is based on observing the interference fringes created when light is incident normally upon a silica glass plate [15,16]. Other techniques include the Abbe's or the Pulfrich's refractometers whose accuracy on the index of refraction is within $\pm 2 \times 10^{-3}$ and $\pm 5 \times 10^{-5}$, respectively [17].

Moreover, when absorption cannot be ignored, both n_λ and k_λ can be retrieved from the directional or hemispherical reflectance and/or emittance of a slab of known thickness. Electromagnetic wave theory can be used to retrieve both n_λ and k_λ, assuming optically smooth surfaces and accounting for internal reflection [18]. Finally, the Kramers–Krönig relations [18] can also be used to predict either the refractive index from the absorption index, or vice versa, at frequency ν [18,19]:

$$n_\nu = 1 + \frac{2}{\pi} P \int_0^\infty \frac{\nu' k_{\nu'}}{\nu'^2 - \nu^2} \, d\nu', \tag{4}$$

$$k_\nu = \frac{-2\nu}{\pi} P \int_0^\infty \frac{n_{\nu'}}{\nu'^2 - \nu^2} \, d\nu', \tag{5}$$

where P denotes the Cauchy principle value of the integral [18]. Alternatively, the refractive and absorption indices can be simultaneously obtained from reflectance. First, the phase angle of the complex reflection coefficient Θ, at frequency ν_0 can be expressed by the Kramers–Krönig relations [20]:

$$\Theta(\nu) = \frac{2\nu}{\pi} P \int_0^\infty \frac{d \ln\sqrt{R(\nu')}}{\nu'^2 - \nu^2} \, d\nu', \tag{6}$$

where $R(\nu)$ is the normal–normal reflectivity expressed as a function of ν:

$$R(\nu) = |r|^2 = \frac{(n_\nu - 1)^2 + k_\nu^2}{(n_\nu + 1)^2 + k_\nu^2}. \tag{7}$$

The Fresnel reflection coefficient r is defined as

$$r = \frac{1 - n_\nu - ik_\nu}{1 + n_\nu + ik_\nu} = |r| e^{i\Theta}. \tag{8}$$

From Eqs. (7) and (8), the refractive and absorption indices can be expressed as

$$n_\nu = \frac{1 - R(\nu)}{1 + R(\nu) - 2\sqrt{R(\nu)} \cos\Theta}, \tag{9}$$

$$k_\nu = \frac{-2\sqrt{R(\nu)} \sin\Theta}{1 + R(\nu) - 2\sqrt{R(\nu)} \cos\Theta}. \tag{10}$$

However, due to the infinite bound of the integrals in Eqs. (4)–(6), these techniques require extrapolations into spectral regions where data are not always available. Furthermore, the integrals need to be computed numerically. Practical limitations and possible errors of Kramers–Krönig relations have been discussed by Riu and Lapaz [19]. These authors concluded that the Kramers–Krönig relations were practically applicable in almost every experimental situation.

B. Absorption Index, k_λ

The value of the absorption index k_λ was not always directly available from the literature and was sometimes recovered from the normal spectral transmittance or emittance data. Indeed, the value of k_λ can be recovered from the normal spectral transmittance $T_{0,\lambda}$, accounting for multiple reflections and expressed as [21]

$$T_{0,\lambda}(L) = \frac{(1 - \rho_\lambda)^2 e^{-\kappa_\lambda L}}{1 - (\rho_\lambda)^2 e^{-2\kappa_\lambda L}}, \tag{11}$$

where L is the thickness of the sample and ρ_λ and κ_λ are the spectral reflectivity of the interface and the spectral absorption coefficient of silica glass, respectively, and are given by

$$\rho_\lambda = \frac{(n_\lambda - 1)^2 + k_\lambda^2}{(n_\lambda + 1)^2 + k_\lambda^2}, \tag{12}$$

$$\kappa_\lambda = \frac{4\pi k_\lambda}{\lambda}. \tag{13}$$

Equations (11)–(13) can be solved as a quadratic in the exponential factor in terms of k_λ. After some algebraic manipulation, one obtains the following expression for k_λ as a function of the refractive index, n_λ, the sample thickness, L, and the spectral normal transmittance, $T_{0,\lambda}$:

$$k_\lambda = -\left(\frac{\lambda}{4\pi L}\right) \ln\left[\frac{\sqrt{(1 - \rho_\lambda)^4 + 4\rho_\lambda^2 T_{0,\lambda}} - (1 - \rho_\lambda)}{2\rho_\lambda^2 T_{0,\lambda}}\right]. \tag{14}$$

Alternatively, the absorption index, k_λ, can also be determined from measurements of the spectral normal emittance, $\epsilon_{\lambda,0}$, by using the following expression [22]:

$$k_\lambda = \left(\frac{\lambda}{4\pi L}\right) \ln\left[\frac{1 - \rho_\lambda - \rho_\lambda \epsilon_{\lambda,0}}{1 - \rho_\lambda - \epsilon_{\lambda,0}}\right]. \tag{15}$$

Note that the above expressions for the absorption index k_λ given by Eqs. (14) and (15) are valid if both $(n_\lambda - 1)$ and $(n_\lambda + 1)$ are much larger than k_λ. In either case, an expression for n_λ is necessary to estimate ρ_λ. As discussed later in this paper, the Sellmeier equation proposed by Malitson [23] can be used for that purpose between 0.21 and 6.7 μm.

In addition, in the UV and IR regions of the spectrum when silica glass is strongly absorbing, most reported values of n_λ and k_λ were retrieved from near-normal reflectance measurements in combination with the Kramers–Krönig relations [24].

3. Experimental Data and Discussion

Table 1 summarizes representative references reporting experimental values of the complex refractive index of silica glass at room temperature for the spectral range from 30 nm to 1000 μm. For each study, the measurement method, the spectral range, as well as the sample thicknesses, compositions, and temperatures investigated are also reported when available. In addition, the absorption index k_λ was derived from transmittance measurements using Eq. (14) if it was not directly reported. Then, computation from transmittance and emittance data sometimes leads to negative values, particularly in the spectral region from 0.2 to 4.0 μm where silica glass is very weakly absorbing. This was the case for transmittance data from [25,26]. Hence, in this region, the experimental data should be used with care since the uncertainty for k_λ is very large and k_λ effectively vanishes.

Figure 1 shows the real and imaginary parts of the refractive index of silica glass, n_λ and k_λ, as a function of wavelength λ over the spectral range from 30 nm to 1000 μm as reported in the references listed in Table 1. Because of the density of data points in some parts of the spectrum and for the sake of clarity, Figs. 2–5 show details of both the real n_λ and imaginary k_λ parts of the complex index of refraction of silica glass for wavelengths between 30 nm and 1 μm, 1 and

Table 1. Summary of the Experimental Data Reporting the Complex Index of Refraction of Silica Glass at Room Temperature[a]

Reference	Wavelength Range (μm)	Measurement Method	Reported Data	Temperature	Sample Thickness	Type	Comments
[11]	7.14–25	Reflection, transmission, Kramers–Krönig relation	n, k	RT	N/A	I	Vitreosil
[12]	2–500	Reflection, Kramers–Krönig method	R, n, k	300, 200, 100, and 10 K	N/A	III	Suprasil, UV grade synthetic fused SiO_2
[13]	7–300	Transmission	n, k	RT	N/A	N/A	
[15]	110–550	Interferometric	T, n, k	RT	2.1409 mm	I	Infrasil (low H_2O)
[16]	3–6.7	Interferometric	n, T	RT	0.23 mm	III	Suprasil 2 ~1000 ppm OH content
[23]	0.21–3.71	Minimum deviation method	n	20 °C	N/A	III	Corning code 7940, Dynasil high-purity synthetic SiO_2 glass and GE type 151
[25]	0.80–2.60	k from Eq. (14)	T	298 K	1.6 mm	N/A	
[26]	0.19–0.42	k from Eq. (14)	T	298 K	2 mm	N/A	
[27]	0.05–0.7	Reflection and Kramers–Krönig	n, ϵ''	RT	N/A	III	Suprasil (UV grade)
[28]	7.19–9.06	Interferometric	n, T, R	RT	0.1956 mm	IV	Suprasil W2
[29]	0.2–3	Reflection and transmission	n, k, R, T	24 °C	N/A	N/A	
[30]	16.7–25	Reflection	R, n, k	RT	N/A	N/A	
[44]	0.35–3.51	Minimum deviation method	n	24 °C	N/A	N/A	Samples from General Electric, Heraeus, Nieder Fused Quartz, and Corning Glass Works
[45]	1.44–4.77	Interferometric	n, T	23.5 °C–481 °C	0.1994 mm	IV	Suprasil W2
[49]	7.14–50	Reflection	n, k	RT	N/A	II	KU and KI
		Kramers–Krönig relation				IV	Impurity did not exceed 0.007%
[50]	0.0006–500		n, k	RT	N/A	N/A	Compilation of data
[51]	1.00–7.5	Transmission	T, κ	RT	5 μm to 3.06 m	N/A	
[54]	0.10–0.16	Reflection and Kramers–Krönig	n, k	RT	N/A	N/A	Samples produced by Electro-Quartz
[55]	1.35–4.85	Interferometric	n, T	23.5 °C	0.2345 mm	IV	Suprasil W2
[56]	8.13–9.63	Reflection	R, n, k	RT	N/A		
[57]	7.84–12.9	Reflection	n, k	RT	N/A		
[58]	0.23–3.37	Minimum deviation method	n	26 °C, 471 °C, and 828 °C	N/A	III	Corning 7940
[59]	7.14–11.11	Reflection, transmission, and Kramers–Krönig relation	n, k	RT	N/A	II	KU
						III	KV
						IV	KI
						I	Infrasil
[60]	7.14–14.29	Reflection	R, k	RT	N/A	N/A	
[61]	0.5–4.5	Minimum deviation	n	RT	N/A	N/A	Sample having low water content supplied by General Electric Company
[62]	0.37, 0.44, 0.55, 1.01, and 1.53	Minimum deviation	n	294, 240, 180, and 120 K	N/A	N/A	
[63]	0.06–40		n, k	RT	N/A	N/A	
[64]	0.2–3.5	Transmission	k, T	RT—1500 °C	0.953 mm	I, III	GE IR type 105, GE UV type 151, and Corning Vycor IR Glass Number 7905
[65]	2.00–6.00	k from Eq. (14)	T	25 °C and 400 °C	2.8 mm	I	GE Type 105
[66]	0.31–3.97	k from Eq. (14)	T	RT	5.45 mm	N/A	

[67]	0.16–0.30	k from Eq. (14)	T	RT	2.04–3.29 mm	III	Corning code 7940 and Dynasil
[68]	1.00–4.62	k from Eq. (14)	T	RT	3.18 mm		
[69]	7.69–11.11	Reflection and Kramers–Krönig	n, k	RT	1.0 mm	II	KU
						III	Optical grade fused quartz
						IV	KI
[70]	7.41–50	Reflection and dispersion analysis[b]	n, k	RT	N/A	IV	KI
[71]	60–560	Transmission and reflection	R, n, k	RT	0.258, 1.05, 2.03, 4.07, 12.35, 12.35, and 25 mm	N/A	$Al_2O_3 \leq 4.0 \times 10^{-3}\%$, $Fe_2O_3 \leq 4.0 \times 10^{-3}\%$, $CaO \leq 2.0 \times 10^{-3}\%$, $Na_2O \leq 1.0 \times 10^{-3}\%$, CuO, TiO_2, MgO, $Mn_3O_4 < 0.001\%$
[72]	83.3–500	Transmission	n, κ	300 K	1.340 ± 0.001 mm		Optically polished
[73]	50–1000	Reflection and transmission	n, k	RT	N/A	N/A	Impurity $\leq 3 \times 10^{-5}$
[74]	100–1000	Transmission	κ	RT	N/A		GE types 101 and 106
[75]	0.029–1.77	Transmission, reflection, and Kramers–Krönig	T, R, n, k	RT	N/A	III	Suprasil I
[76]	100–667	Transmission	κ	100 and 300 K			GE type 101
[77]	7.69–11.1	Internal reflection and Kramers–Krönig	n, k	RT	N/A	III	KU-1 glass, broken surface
[78]	2–35	Reflection and Kramers–Krönig	T, R, n, k	RT	N/A	N/A	

[a]RT is room temperature.
[b]Reference [24].

15 μm, 15 and 100 μm, and 100 and 1000 μm, respectively.

Overall, the reported values for both the real and imaginary parts of the complex index of refraction agree relatively well. Studies showing large deviations from other studies suggest that the data are unreliable [24]. For example, data reported by Ellis *et al.* [27] strongly disagree with all other data between 60 nm and the visible. Locations of extrema of n_λ are consistent among all experimental data except for those reported by Tan [28] ($7.19\ \mu m \leq \lambda \leq 9.06\ \mu m$), Khashan and Nassif [29] ($0.2\ \mu m \leq \lambda \leq 3.0\ \mu m$), and Reitzel [30] ($16.7\ \mu m \leq \lambda \leq 25\ \mu m$). The data for wavelengths below 9 μm as reported by various authors agree well with one another. However, the data agree considerably less for wavelengths between 9 and 50 μm. Beyond 50 μm, a smaller number of values for n_λ have been reported, but the data agree relatively well.

Furthermore, trends and the locations of extrema in the measured absorption index are consistent from one study to another. However, discrepancies larger than those for n_λ can be observed in reported data for k_λ in some parts of the spectrum. They are most likely due to (i) the impurity of the sample (e.g., OH group, alkali, metallic content), (ii) the presence of inclusions, bubbles, or point defects, (iii) the sample preparation and surface optical quality, and/or (iv) the uncertainty in the measurement and retrieval techniques. Note that the flatness of the sample surface becomes a critical parameter in the visible and UV [31,32]. In this wavelength range, the surface roughness must remain much smaller than the wavelength to avoid surface scattering and consider the surface as optically smooth.

The imaginary part of the complex refractive index of silica glass k_λ is small from the near UV to the near-IR part of the spectrum. Practically, silica glass is transparent from 200 nm up to 3.5–4.0 μm. In the extreme UV (for wavelengths below 200 nm) and in the IR and far-IR (beyond 4.0) silica glass can be considered opaque. In the UV region of the spectrum below 200 nm, the strong absorption of silica glass is caused by the interaction of the electromagnetic radiation with electrons of Si—O bonds [17] and with structural imperfections or point defects such as OH groups, Si—Si bonds, and strained Si—O—Si bonds [33]. This results in a sharp UV cutoff (also called the absorption edge) at ~160 nm [17,34]. The location of the absorption edge depends on the glass composition, impurity level, and point defects formed during the manufacturing process [17,33] as well as on temperature [35]. For example, it is shifted toward the visible wavelengths due to the presence of impurities in particular ions Fe^{3+}, Cr^{3+}, and Ti^{3+} [36]. Similar effects are observed when increasing the alkali contents [34] or the temperature [35]. On the contrary, the absorption edge is slightly shifted to lower wavelengths for crystal quartz [34]. Shifting the absorption edge to lower wavelengths (even slightly) has been the subject of intense studies to enable the use

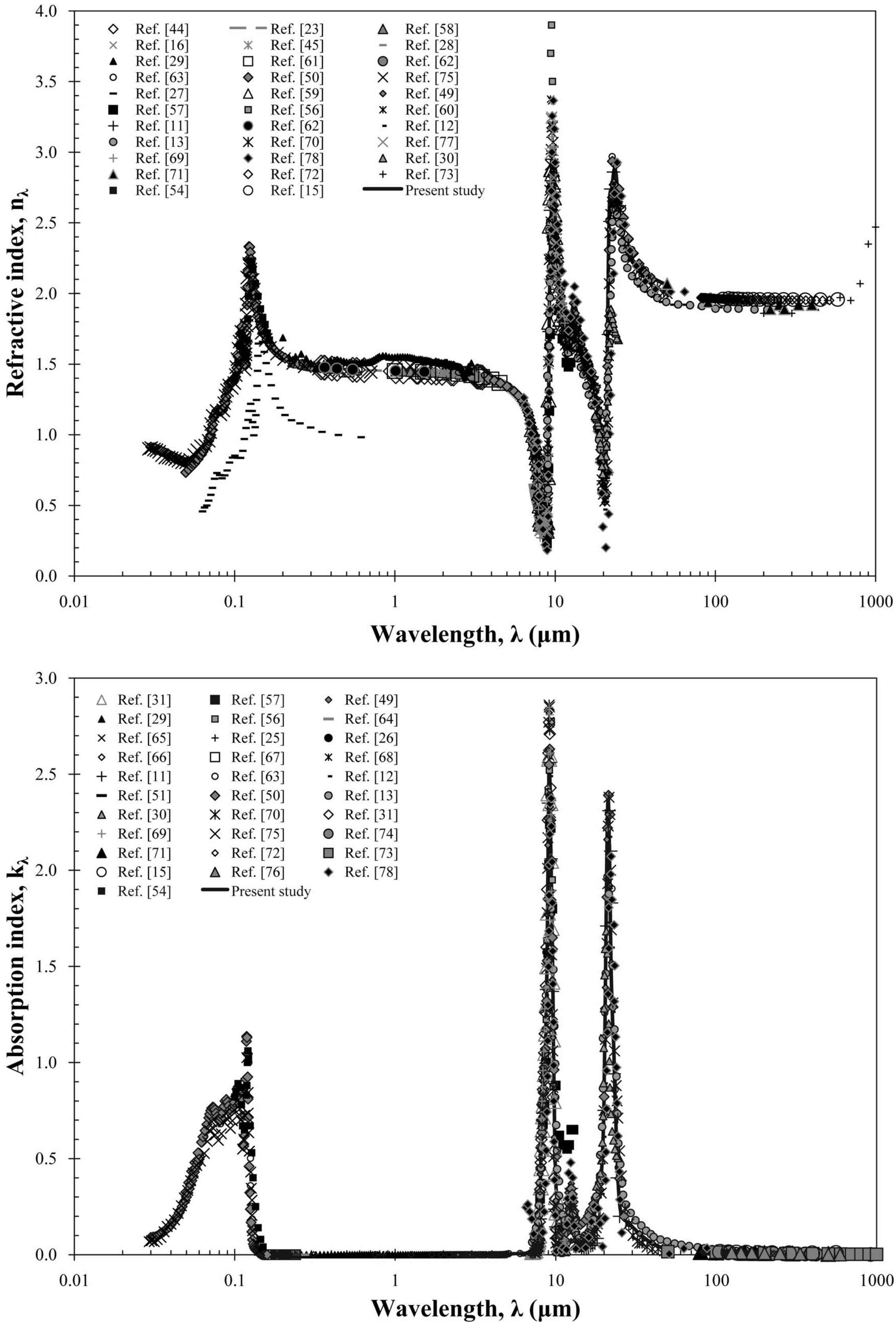

Fig. 1. Real n_λ and imaginary k_λ parts of the complex refractive index of silica glass reported in the literature and summarized in Table 1. The solid curve (present study) was obtained with Eqs. (21)–(24) by using coefficients listed in Table 2.

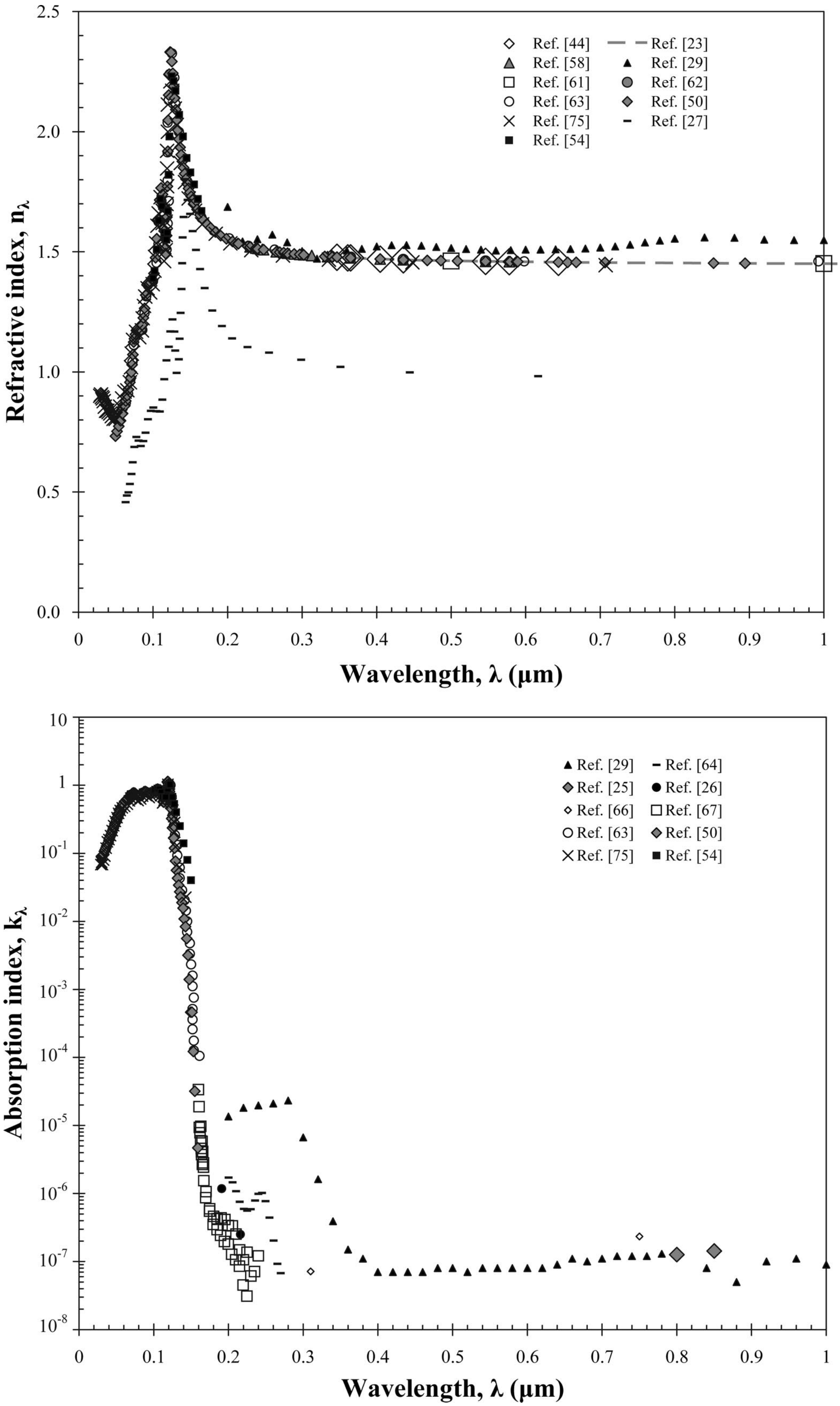

Fig. 2. Real n_λ and imaginary k_λ parts of the complex refractive index of silica glass between 30 nm and 1 μm as reported in the literature and summarized in Table 1.

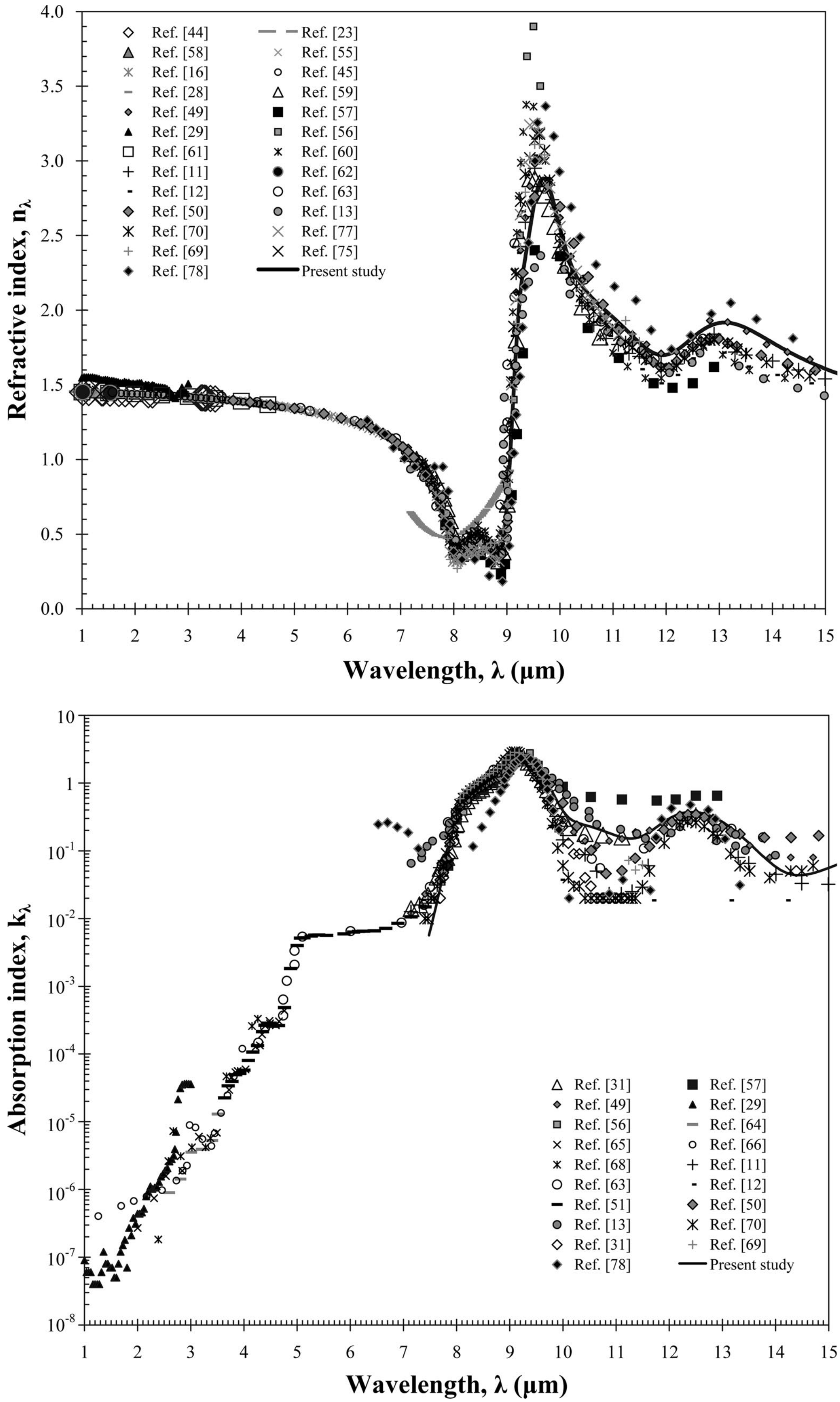

Fig. 3. Real n_λ and imaginary k_λ parts of the complex refractive index of silica glass between 1 and 15 μm as reported in the literature and summarized in Table 1. The solid curve (present study) was obtained with Eqs. (21)–(24) by using coefficients listed in Table 2.

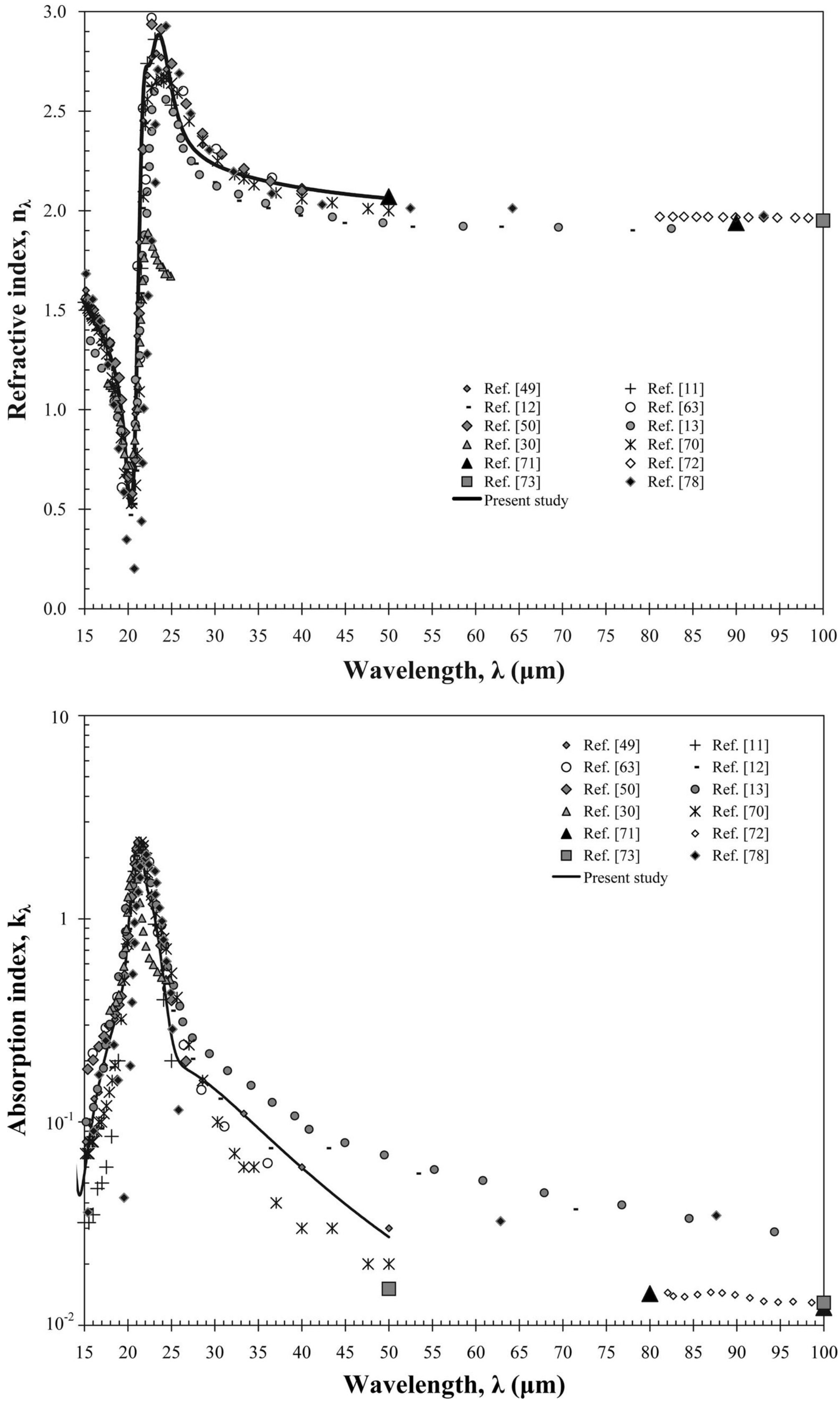

Fig. 4. Real n_λ and imaginary k_λ parts of the complex refractive index of silica glass between 15 and 100 μm as reported in the literature and summarized in Table 1. The solid curve (present study) was obtained with Eqs. (21)–(24) by using coefficients listed in Table 2.

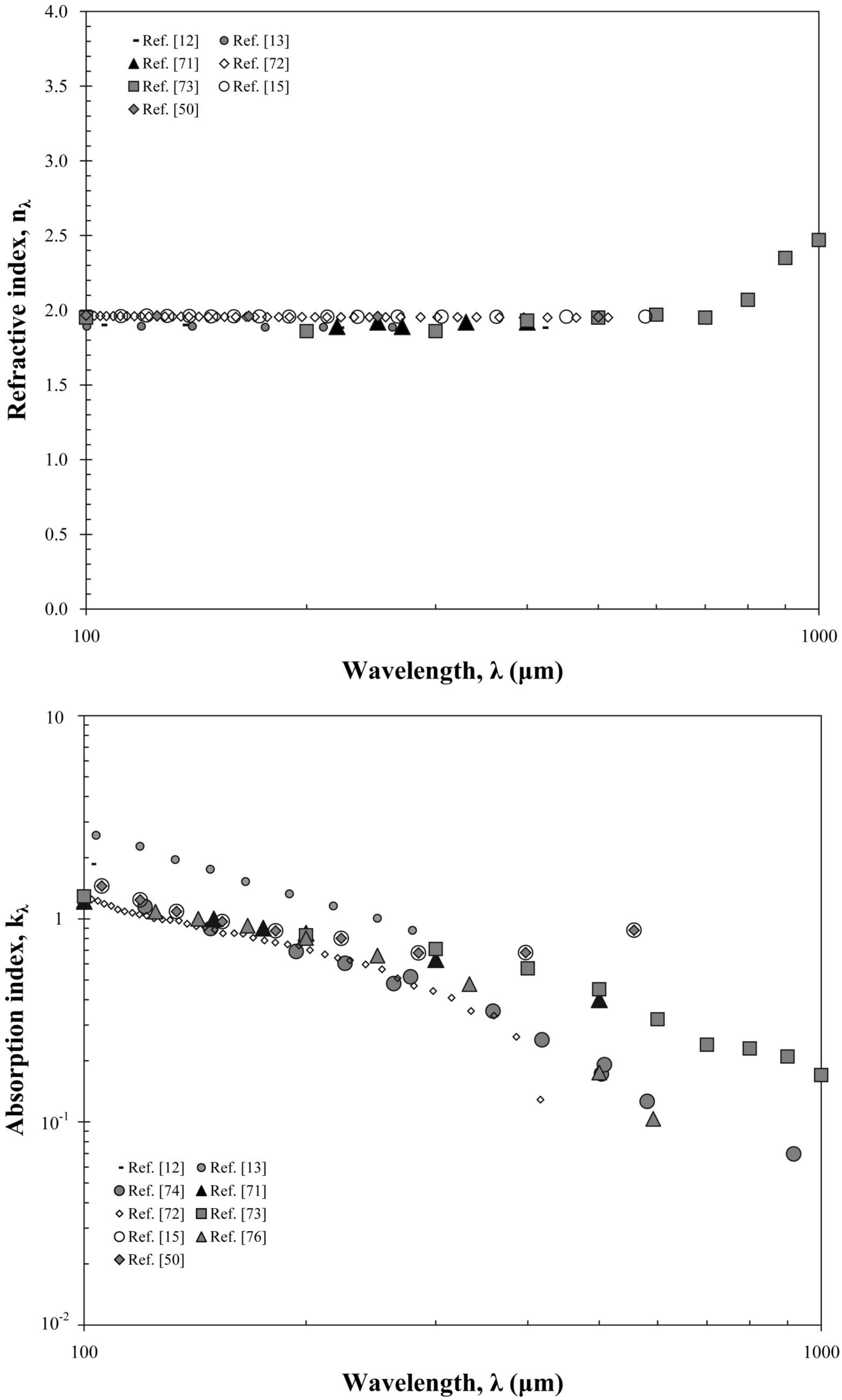

Fig. 5. Real n_λ and imaginary k_λ parts of the complex refractive index of silica glass between 100 and 1000 μm as reported in the literature and summarized in Table 1.

of silica glass for photomask material in 157 nm photolithography using F_2 excimer lasers [32,37,38]. An acceptable transmittance at $\sim$157 nm has been achieved by minimizing the OH content of silica [37] or by doping silica glass with network modifiers such as fluorine, which relaxes the glass structure and eliminates strained Si—O—Si bonds [33]. Experimental measurements and theoretical calculations of the electronic structure of SiO_2 has been reviewed by Griscom [39] and spectroscopic data for wavelengths between 90 and 350 nm have been discussed by Sigel [34]. An interaction between the UV radiation and electrons and point defects is also responsible for the steep increase of n_λ for wavelengths less than 300 nm.

In the IR part of the spectrum, silica glass is effectively opaque for a wavelength larger than 3.5–4.0 μm. Beyond this wavelength, three major absorption bands can be observed (Fig. 1) due to the resonance of Si—O—Si vibrations. The absorption peak between 9.0 and 9.5 μm can be attributed to the asymmetric stretching vibration of Si—O—Si bridges [17,24]. The absorption band at $\sim$12.5 μm is due to the symmetric vibration stretching of the Si—O—Si bridge involving the displacement of the O atom perpendicular to the Si—Si direction in the Si—O—Si plane [24]. The third band between 21 and 23 μm is the consequence of the O—Si—O bending vibration but has also been attributed to the "rocking" mode of Si—O—Si bonds caused by the displacement of an oxygen atom out of the Si—O—Si plane [24]. The resonance of Si—O—Si vibrations are also responsible for the sharp decreases in n_λ around the resonance wavelengths [17]. The reader is referred to [24, pp. 63–77] for a detailed discussion on vibrational spectroscopy of silica glass at these wavelengths. Moreover, smaller absorption bands at $\sim$ wavelengths 2.73–2.85, 3.5, and 4.3 μm correspond to the presence of OH groups in the structure of the glass [17,40–42]. The magnitude of the absorption depends on the melting technology and in particular on the partial pressure of water vapor above the melt during the melting process [17]. The concentration of OH groups in silica glass can be computed from the absorption band at $\sim$ wavelength 2.73–2.85 μm [17]. To the best of our knowledge, no model or approximate equation has been proposed for the absorption index of silica glass. This is the subject of Section 4.

4. Optical Constant Theory

The complex index of refraction, $m_\lambda = n_\lambda + ik_\lambda$, and the complex relative dielectric permittivity, $\epsilon(\lambda) = \epsilon'(\lambda) + i\epsilon''(\lambda)$ are related by the expression $\epsilon(\lambda) = m_\lambda^2$, i.e., [21]

$$\epsilon'(\lambda) = n_\lambda^2 - k_\lambda^2, \qquad \epsilon''(\lambda) = 2n_\lambda k_\lambda. \tag{16}$$

Numerous physical models such as the Lorentz model, the Drude model, and the Debye relaxation model have been proposed to predict the optical properties of solids [18]. The Lorentz model assumes that electrons and ions in the material are harmonic oscillators subject to the force applied by time-dependent electromagnetic fields. Then the complex relative dielectric permittivity can be expressed in terms of frequency ν as follows [21]:

$$\begin{aligned}\epsilon(\nu) &= 1 + \sum_j \frac{\nu_{pj}^2}{\nu_j^2 - \nu^2 - i\gamma_j\nu} \\ &= 1 + \sum_j \frac{\nu_{pj}^2(\nu_j^2 - \nu^2) + i\gamma_j\nu_{pj}^2\nu}{(\nu_j^2 - \nu^2)^2 + \gamma_j^2\nu^2},\end{aligned} \tag{17}$$

where ν_{pj} and ν_j are the plasma and resonance frequencies, respectively. The parameter γ_j is the damping factor of the oscillators. Only when ν is very close to one of the resonance frequencies ν_j, the imaginary terms in Eq. (17) are important [43]. Thus, $\gamma_j\nu$ are negligibly small compared with $(\nu_j^2 - \nu^2)$ for silica glass for a wavelength below 7 μm and ϵ'' is virtually equal to 0.0. Hence, after substituting Eq. (2) into Eq. (17), ϵ can be expressed in terms of λ as follows:

$$\epsilon(\lambda) = \epsilon'(\lambda) = 1 + \sum_j \frac{A_j^2\lambda^2}{(\lambda^2 - \lambda_j^2)}, \tag{18}$$

where $A_j = \nu_{pj}\lambda_j/c_\lambda$ with λ_j being the resonance wavelength. Moreover, as $\epsilon''(\lambda)$ vanishes, the medium is weakly absorbing and k_λ is negligibly small compared with n_λ. Then $\epsilon'(\lambda)$ is equal to n_λ^2 and given by the Sellmeier dispersion formula:

$$\epsilon'(\lambda) = n_\lambda^2 = 1 + \sum_j \frac{A_j^2\lambda^2}{(\lambda^2 - \lambda_j^2)}. \tag{19}$$

Different formulas for the refractive index of silica glass as a function of wavelength and based on the Sellmeier dispersion formula have been proposed in the literature [23,44,45] for different spectral regions. Rodney and Spindler [44] suggested a formula for n_λ over a spectral range from 0.347 to 3.508 μm at 31 °C while Tan and Arndt [45] proposed another equation in the spectral region from 1.44 to 4.77 μm at temperatures ranging from 23.5 to 481 °C. In addition, for the spectral range from 0.21 to 3.71 μm at 20 °C, Malitson [23] fitted experimental data with the following three-term Sellmeier equation:

$$\begin{aligned}n_\lambda^2 = 1 &+ \frac{0.6961663\lambda^2}{\lambda^2 - (0.0684043)^2} + \frac{0.4079426\lambda^2}{\lambda^2 - (0.1162414)^2} \\ &+ \frac{0.8974794\lambda^2}{\lambda^2 - (9.896161)^2}.\end{aligned} \tag{20}$$

Tan [16] confirmed the validity of Eq. (20) for wavelengths up to 6.7 μm. Furthermore, for a spectral range over 8 μm, an approximate piecewise linear fit was given by Dombrovsky [46]. However, no physics-

Table 2. Parameters Used to Interpolate the Refractive Index n_λ and Absorption Index k_λ of Silica Glass by Using Eqs. (21)–(24)[a,b]

j	α_j	η_{0j}	σ_j
1	3.7998	1089.7	31.454
2	0.46089	1187.7	100.46
3	1.2520	797.78	91.601
4	7.8147	1058.2	63.153
5	1.0313	446.13	275.111
6	5.3757	443.00	45.220
7	6.3305	465.80	22.680
8	1.2948	1026.7	232.14

[a] $\epsilon_\infty = 2.1232$.
[b] These parameters were obtained by fitting the equations to data of Popova *et al.* [49].

based formulas have been developed for the spectral range beyond 8 μm.

In parts of the spectrum where k_λ cannot be neglected or when the frequency ν is very close to the resonance frequencies, the Sellmeier equation for n_λ is no longer valid and an alternative model must be used. Recently, Meneses *et al.* [47] proposed a new dielectric function model based on the causal version of the Voigt function. The model was validated by fitting the IR spectra of two different glasses and confirmed to be more appropriate than the Lorentz model [47]. Moreover, the authors proposed another simplified model based on Gaussian functions [48]. Then, the dielectric constant can be written as

$$\epsilon(\eta) = \epsilon'(\eta) + i\epsilon''(\eta) = \epsilon_\infty + \sum_j \left[g_{cj}^{kkg}(\eta) + i g_{cj}(\eta)\right], \tag{21}$$

where the high frequency dielectric constant is denoted by ϵ_∞. In addition, the Gaussian functions $g_{cj}(\eta)$ and $g_{cj}^{kkg}(\eta)$ are defined as

$$g_{cj}(\eta) = \alpha_j \exp\left[-4\ln 2\left(\frac{\eta-\eta_{0j}}{\sigma_j}\right)^2\right] - \alpha_j \times \exp\left[-4\ln 2\left(\frac{\eta+\eta_{0j}}{\sigma_j}\right)^2\right], \tag{22}$$

$$g_{cj}^{kkg}(\eta) = \frac{2\alpha_j}{\pi}\left[D\left(2\sqrt{\ln 2}\,\frac{\eta+\eta_{0j}}{\sigma_j}\right) - D\left(2\sqrt{\ln 2}\,\frac{\eta-\eta_{0j}}{\sigma_j}\right)\right]. \tag{23}$$

Here, α_j is the amplitude, η_{0j} is the peak position, σ_j is the full width at half-maximum, and $D(x)$ is an operator defined as

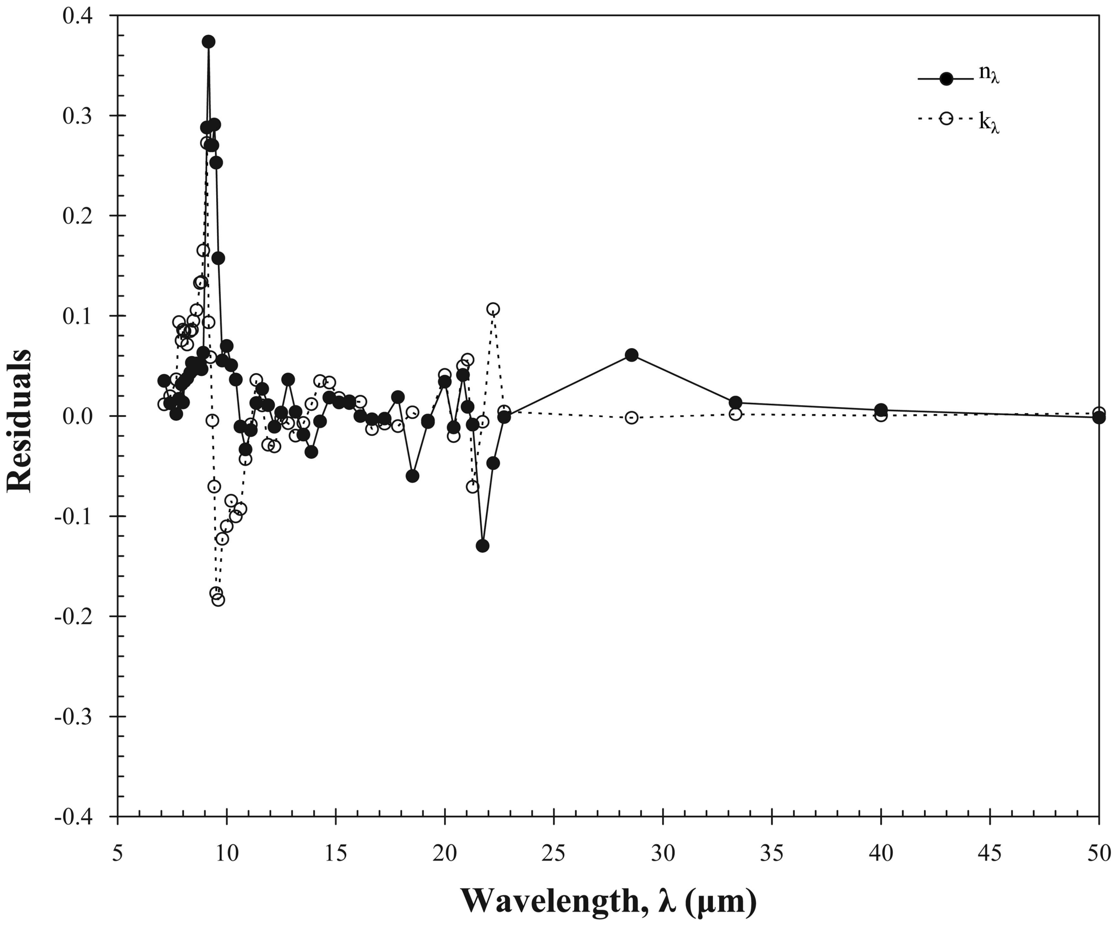

Fig. 6. Residuals between experimental [49] and predicted values of n_λ and k_λ. The predicted values are based on Eqs. (21)–(24) with coefficients listed in Table 2.

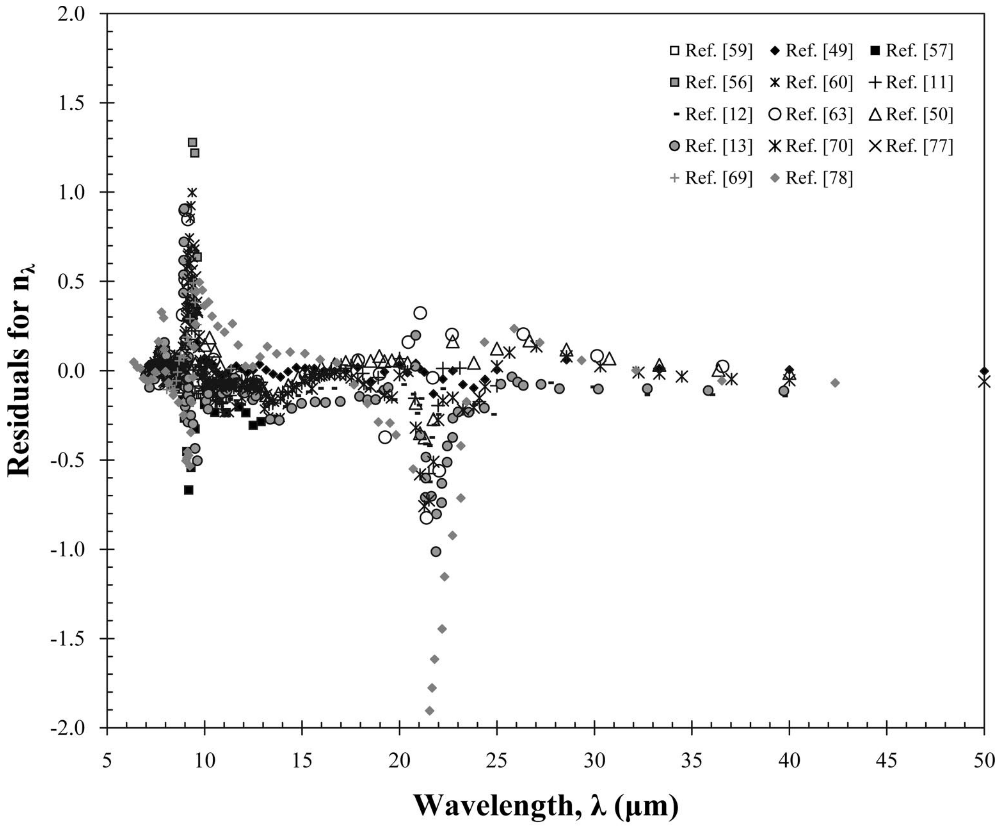

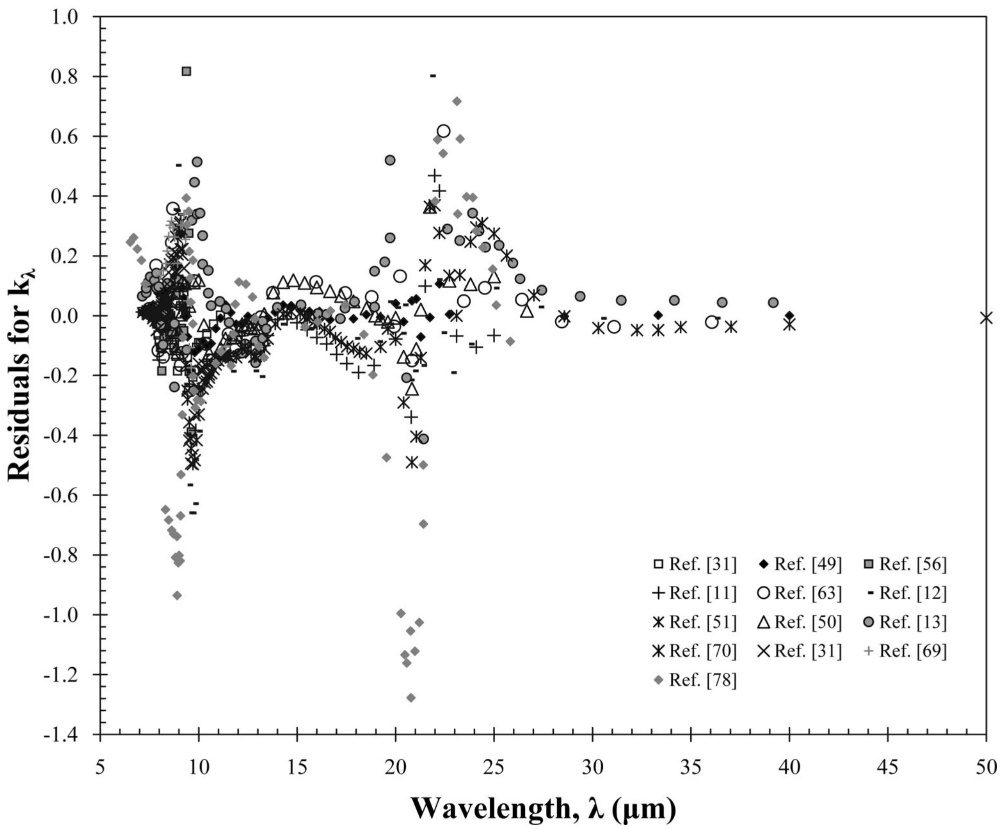

Fig. 7. Residuals between the experimental data on the refractive index and absorption index and values predicted in this work by using Eqs. (21)–(24) along with coefficients listed in Table 2.

$$D(x) = e^{-x^2}\int_0^x e^{t^2}\mathrm{d}t. \tag{24}$$

In the present study, this model is used to interpolate the refractive index n_λ and absorption index k_λ for wavelengths λ between 7 and 50 μm. It enables one to describe the experimental data with a reduced set of parameters [48] over a wide spectral range, including the spectral range where k_λ may be large. Note that the above simplified model satisfies the Kramers–Krönig relation.

The practical procedure for fitting complex refractive index data conducted in this paper is as follows: (i) the spectral reflectivity at normal incidence, $R(\eta)$, is computed from Eq. (7), (ii) parameters of $\epsilon(\eta)$ in Eqs. (21) and (22) are determined by curve fitting for $R(\eta)$ expressed as

$$R(\eta) = \left|\frac{\sqrt{\epsilon(\eta)} - 1}{\sqrt{\epsilon(\eta)} + 1}\right|^2, \tag{25}$$

and (iii) n_η and k_η are computed using Eq. (16). The advantage of this procedure is that (a) fitting the reflectivity is easier than fitting n_λ and k_λ independently, (b) both n_λ and k_λ can be derived from a single curve fitting, and (c) the result automatically satisfies the Kramers–Krönig relations.

The experimental data of Popova *et al.* [49] were selected to develop formulas for both n_λ and k_λ because these data cover a wide spectral range from 7 to 50 μm, and both the refractive and absorption indices are reported at the same wavelength enabling the calculation of $R(\eta)$. In the spectral region from 0.2 to 7 μm, the absorption index of silica glass is very small and may be assumed to be zero for all practical purposes as suggested by Fig. 1. Moreover, reported data, including that of Popova *et al.* [49], indicates that the refractive index is satisfactorily predicted by the Sellmeier formula reported by [16] and Malitson [23] between 0.2 and 7 μm and given by Eq. (20). Therefore, the present study focuses on the spectral range between 7 and 50 μm.

To fit the model with experimental data, the FOCUS software was used [47,48]. By adding terms in Eq. (21) one by one, eight terms were found to best fit the experimental data. The fitting curves obtained in this study are shown in Figs. 3 and 4, and the associated parameters α_j, η_{0j}, and σ_j used in Eqs. (21)–(23) are summarized in Table 2. The fitting curves for n_λ and k_λ obtained in the present study agree well with the data of Popova *et al.* [49] and with most of other data shown in Figs. 3 and 4. The differences (or residuals) between the data of Popova *et al.* [49] and the model predictions for both n_λ and k_λ using the parameters given in Table 2 are shown in Fig. 6. It indicates that the residuals are less than 0.06 except near 9 and 22.5 μm, where they reach up to 0.3 around 9 μm and 0.14 around 22.5 μm. This can be attributed to the fact that the refractive index changes greatly in those wavelength regions. However, these residuals are small compared with much larger difference observed in the experimental data reported for n_λ. For example, one can see differences larger than 0.5 among reported refractive index data in the spectral range between 9 and 10 μm. Thus, the approximation obtained here is acceptable and can be useful in engineering applications.

Moreover, the residuals between the experimental data for the refractive and absorption indices listed in Table 1, and the model predictions using the parameters given in Table 2 are shown in Fig. 7. Here again, the residuals are less than 0.3 except at ~9.0 and 22.5 μm. This indicates that the model predictions using the parameters given in Table 2 agree with all data reported in the literature at the spectral range except at ~9 and 22.5 μm. However, large discrepancies in reported experimental data sets can be observed around these two wavelengths. In general, the model should be used with care when applied outside the spectral range from 0.2 to 50 μm.

Finally, given its widespread use, particular attention was paid to the compilation of data reported by Philipp [50] for the refractive and absorption indices of silica glass over the spectral range from 0.006 to 500 μm. The compilation consists of experimental data reported by various authors [15,20,51–54] as well as unpublished data. Philipp [50] also retrieved optical properties from the absorption coefficient as well as computer generated values. Qualitatively, good agreement between the data compiled by Philipp [50] and the other data is observed in Figs. 2–5. Moreover, residuals with the present model range from -0.42 to 0.19 for n_λ and -0.25 to 0.37 for k_λ from 7 to 50 μm.

5. Conclusions

A thorough review of experimental data for the complex refractive index of silica glass at near room temperatures over a spectral range from 30 nm to 1000 μm implies that the values reported in the literature can vary significantly due to numerous sample features and experimental methods and conditions. Hence, it is essential to report the silica glass synthesis method, composition, impurity, and defects level, sample thickness, surface roughness, and temperatures as well as the retrieval method and the underlying assumptions when one reports optical properties of glass. However, the general features of the complex refractive index spectra are relatively consistent throughout the region of the spectrum considered. Silica glass is effectively opaque for wavelengths shorter than 200 nm and larger than 3.5–4.0 μm. Strong absorption bands are observed (i) below 160 nm due to interaction with electrons, absorption by impurities, and the presence of OH groups and point defects, (ii) at ~2.73–2.85, 3.5, and 4.3 μm also caused by OH groups, (ii) at ~9–9.5, 12.5, and 21–23 μm due to Si—O—Si resonance modes of vibration. New formulas for both the real and imaginary parts of the complex refractive index are proposed over a wide spectral range between 7 and 50 μm, thus complementing the existing analytical formula for n_λ in the range of 0.21–7 μm [16,23]. The imaginary part of the complex refractive index can be neglected in much of this range (0.21–4 μm). The differences between various experimental data are comparable and greater than the differences between the results of these formulas and the experimental data used to develop them. Hence it is believed that the formulas proposed are useful for practical engineering applications such as simulations and optimizations of optical and thermal systems. The data collected and presented in this study are available in digital form online [79] or directly from the corresponding author upon request.

The authors thank Asahi Glass Co., Ltd. Japan for financial support. They are grateful to D. De Sousa Meneses for helpful discussion about FOCUS. The contribution of M. Jonasz was supported by MJC Optical Technology.

References

1. G. Hart, "The nomenclature of silica," Am. Mineral. **12,** 383–395 (1927).
2. R. B. Sosman, *The Phase of Silica* (Rutgers U. Press, 1964).
3. G. Hetherington, K. H. Jack, and M. W. Ramsay, "The high-temperature electrolysis of vitreous silica, part I. Oxidation, ultra-violet induced fluorescence, and irradiation colour," Phys. Chem. Glasses **6,** 6–15 (1965).
4. R. Bruckner, "Properties and structure of vitreous silica. I," J. Non-Cryst. Solids **5,** 123–175 (1970).
5. K. M. Davis, A. Agarwal, M. Tomozawa, and K. Hirao, "Quantitative infrared spectroscopic measurement of hydroxyl concentrations in silica glass," J. Non-Cryst. Solids **203,** 27–36 (1996).
6. R. H. Doremus, *Glass Science* (Wiley, 1994).
7. J. M. Senior, *Optical Fiber Communications: Principles and Practice,* 2nd ed. (Prentice Hall, 1992).
8. G. E. Keiser, *Optical Fiber Communications,* 3rd ed. (McGraw-Hill Higher Education—International Editions: Electrical Engineering Series, 2000).
9. B. Brixner, "Refractive-index interpolation for fused silica," J. Opt. Soc. Am. **57,** 674–676 (1967).
10. L. E. Sutton and O. N. Stavroudis, "Fitting refractive index data by least squares," J. Opt. Soc. of Am. **51,** 901–905 (1961).
11. T. Steyer, K. L. Day, and R. Huffman, "Infrared absorption by small amorphous quartz spheres," Appl. Opt. **13,** 1586–1590 (1974).
12. T. Henning and H. Mutschke, "Low-temperature infrared properties of cosmic dust analogues," Astron. Astrophys. **327,** 743–754 (1997).
13. C. Koike, H. Hasegawa, N. Asada, and T. Komatuzaki, "Optical constants of fine particles for the infrared region," Mon. Not. R. Astron. Soc. **239,** 127–137 (1989).
14. M. Born and E. Wolf, *Principles of Optics,* 7th ed. (Cambridge U. Press, 1999).
15. C. M. Randall and R. D. Rawcliffe, "Refractive indices of germanium, silicon, and fused quartz in the far infrared," Appl. Opt. **6,** 1889–1895 (1967).
16. C. Tan, "Determination of refractive index of silica glass for infrared wavelengths by IR spectroscopy," J. Non-Cryst. Solids **223,** 158–163 (1998).
17. I. Fanderlik, "Glass science and technology," *Optical Properties of Glass* (Elsevier Science, 1983), Vol. 5.
18. C. F. Bohren and D. R. Huffman, *Absorption and Scattering of Light by Small Particles* (Wiley, 1983).
19. P. J. Riu and C. Lapaz, "Practical limits of the Kramers–Krönig relationships applied to experimental bioimpedance data," Ann. N.Y. Acad. Sci. **873,** 374–380 (1999).
20. H. Philipp, "The infrared optical properties of SiO_2 and SiO_2 layers on silicon," J. Appl. Phys. **50,** 1053–1057 (1979).
21. M. F. Modest, *Radiative Heat Transfer* (Academic, 2003).
22. A. V. Dvurechensky, V. Petrov, and V. Y. Reznik, "Spectral emissivity and absorption coefficient of silica glass at extremely high temperatures in the semitransparent region," Infrared Phys. **19,** 465–469 (1979).
23. I. Malitson, "Interspecimen comparison of the refractive index of fused silica," J. Opt. Soc. Am. **55,** 1205–1209 (1965).
24. A. M. Efimov, *Optical Constants of Inorganic Glasses* (CRC, 1995).
25. L. Bogdan, "Measurement of radiative heat transfer with thin-film resistance thermometers," NASA CR **27,** 1–39 (1964).
26. A. Sviridova and N. Suikovskaya, "Transparent limits of interference films of hafnium and thorium oxides in the ultraviolet region of the spectrum," Opt. Spectrosc. **22,** 509–512 (1967).
27. E. Ellis, D. W. Johnson, A. Breeze, P. M. Magee, and P. G. Perkins, "The electronic structure and optical properties of oxide glasses I. SiO_2, Na_2O:SiO_2 and Na_2O:CaO:SiO_2," Philos. Mag. B **40,** 105–124 (1979).
28. C. Tan, "Optical interference and refractive index of silica glass in the infrared absorption region," J. Non-Cryst. Solids **249,** 51–54 (1999).
29. M. Khashan and A. Nassif, "Dispersion of the optical constants of quartz and polymethyl methacrylate glasses in a wide spectral range: 0.2–3 μm," Opt. Commun. **188,** 129–139 (2001).
30. J. Reitzel, "Infrared spectra of SiO_2 from 400 cm^{-1} to 600 cm^{-1}," J. Chem. Phys. **23,** 2407–2409 (1955).
31. G. M. Mansurov, R. K. Mamedov, S. Sudarushkin, V. K. Sidorin, K. K. Sidorin, V. I. Pshenitsyn, and V. M. Zolotarev, "Study of the nature of a polished quartz-glass surface by ellipsometric and spectroscopic methods," Opt. Spectrosc. **52,** 852–857 (1982).
32. Y. Ikuta, S. Kikugawa, T. Kawahara, H. Mishiro, N. Shimodaira, and S. Yoshizawa, "New silica glass AQF for 157-nm lithography," Proc. SPIE **4000,** 1510–1514 (2000).
33. K. Kajihara, "Improvement of vacuum-ultraviolet transparency of silica glass by modification of point defects," J. Ceram. Soc. Jpn. **115,** 85–91 (2007).
34. G. H. Sigel, "Ultraviolet spectra of silicate glasses: a review of some experimental evidence," J. Non-Cryst. Solids **13,** 372–398 (1974).
35. N. Shimodaira, K. Saito, A. Ikushima, T. Kamihori, and S. Yoshizawa, "UV transmittance of fused silica glass influenced by thermal disorder," Proc. SPIE **4000,** 1553–1559 (2000).
36. H. Rawson, "Glass science and technology," *Properties and Applications of Glass* (Elsevier Science, 1980), Vol. 3.
37. C. M. Smith and L. A. Moore, "Fused silica for 157-nm transmittance," Proc. SPIE **3676,** 834–841 (1999).
38. Y. Ikuta, S. Kikugawa, T. Kawahara, H. Mishiro, K. Okada, K. Ochiai, K. Hino, T. Nakajima, M. Kawata, and S. Yoshizawa, "New modified silica glass for 157-nm lithography," Proc. SPIE **4066,** 564–570 (2000).
39. D. Griscom, "The electronic structure of SiO_2: a review of recent spectroscopic and theoretical advances," J. Non-Cryst. Solids **24,** 155–234 (1977).
40. V. Petrov and S. Stepanov, "Radiation characteristics of quartz glasses spectral radiating power," Teplofiz. Vys. Temp. **13,** 335–345 (1975).
41. V. Plotnichenko, V. Sokolov, and E. Dianov, "Hydroxyl groups in high-purity silica glass," J. Non-Cryst. Solids **261,** 186–194 (2000).

42. A. M. Efimov and V. G. Pogareva, “IR absorption spectra of vitreous silica and silicate glasses: The nature of bands in the 1300 to 5000 cm^{-1} region,” Chem. Geol. **229,** 198–217 (2006).
43. D. J. Griffiths, *Introduction to Electrodynamics,* 3rd ed. (Prentice Hall, 1999).
44. W. Rodney and R. Spindler, “Index of refraction of fused quartz for ultraviolet, visible, and infrared wavelengths,” J. Opt. Soc. Am. **44,** 677–679 (1954).
45. C. Tan and J. Arndt, “Temperature dependence of refractive index of glass SiO_2 in the infrared wavelength range,” J. Phys. Chem. Solids **61,** 1315–1320 (2000).
46. L. Dombrovsky, “Quartz-fiber thermal insulation: infrared radiative properties and calculation of radiative-conductive heat transfer,” J. Heat Transfer **118,** 408–414 (1996).
47. D. D. S. Meneses, G. Gruener, M. Malki, and P. Echegut, “Causal Voigt profile for modeling reflectivity spectra of glasses,” J. Non-Cryst. Solids **351,** 124–129 (2005).
48. D. D. S. Meneses, M. Malki, and P. Echegut, “Structure and lattice dynamics of binary lead silicate glasses investigated by infrared spectroscopy,” J. Non-Crystal. Solids **352,** 769–776 (2006).
49. S. Popova, T. Tolstykh, and V. Vorobev, “Optical characteristics of amorphous quartz in the 1400–200 cm^{-1} region,” Opt. Spectrosc. **33,** 444–445 (1972).
50. H. R. Philipp, “Silicon dioxide (SiO_2) glass,” in *Handbook of Optical Constants of Solids,* E. D. Palik, ed. (Academic, 1985), Vol. I, pp. 749.
51. D. G. Drummond, “The infra-red absorption spectra of quartz and fused silica from 1 to 7.5 μ II—experimental results,” Proc. R. Soc. London Ser. A **153,** 328–339 (1936).
52. H. R. Philipp, “Optical transitions in crystalline and fused quartz,” Solid State Commun. **4,** 73–75 (1966).
53. H. R. Philipp, “Optical properties of non-crystalline Si, SiO, SiO_x and SiO_2,” J. Phys. Chem. Solids **32,** 1935–1945 (1971).
54. P. Lamy, “Optical constants of crystalline and fused quartz in the far ultraviolet,” Appl. Opt. **16,** 2212–2214 (1977).
55. C. Tan and J. Arndt, “Refractive index, optical dispersion, and group velocity of infrared wave in silica glass,” J. Phys. Chem. Solids **62,** 1087–1092 (2001).
56. C. Boeckner, “A method of obtaining the optical constants of metallically reflecting substances in the infrared,” J. Opt. Soc. Am. **19,** 7–15 (1929).
57. O. Girin, Y. Kondratev, and E. Raaben, “Optical constants and spectral microcharacteristics of NaO_2–SiO_2 glasses in the IR region of the spectrum,” Opt. Spectrosc. **29,** 397–403 (1970).
58. J. Wray and J. Neu, “Refractive index of several glasses as a function of wavelength and temperature,” J. Opt. Soc. Am. **59,** 774–776 (1969).
59. V. Zolotarev, “The optical constants of amorphous SiO_2 and GeO_2 in the valence band region,” Opt. Spectrosc. **29,** 34–37 (1970).
60. I. Simon and H. McMahon, “Study of the structure of quartz, cristobalite, and vitreous silica by reflection in infrared,” J. Chem. Phys. **21,** 23–30 (1953).
61. M. Herzberger and C. Salzberg, “Refractive indices of infrared optical materials and color correction of infrared lenses,” J. Opt. Am. **52,** 420–427 (1962).
62. T. Yamamuro, S. Sato, T. Zenno, N. Takeyama, H. Matsuhara, I. Maeda, and Y. Matsueda, “Measurement of refractive indices of 20 optical materials at low temperatures,” Opt. Eng. **45,** 083401 (2006).
63. H. Bach and N. Neuroth, eds., *The Properties of Optical Glass,* 2nd ed. (Springer-Verlag, 2004).
64. E. Beder, C. Bass, and W. Shackleford, “Transmittivity and absorption of fused quartz between 0.2 and 3.5 μm from room temperature to 1500 °C,” J. Am. Ceram. Soc. **10,** 2263–2268 (1971).
65. D. Gillespie, A. Olsen, and L. Nichols, “Transmittance of optical materials at high temperatures in the 1-μ to 12-μ range,” Appl. Opt. **4,** 1488–1493 (1965).
66. G. Calingaert, S. Heron, and R. Stair, “Sapphire and other new combustion-chamber window materials,” SAE J. **39,** 448–450 (1936).
67. D. Heath and P. Sacher, “Effects of a simulated high-energy space environment on the ultraviolet transmittance of optical material between 1050 Å and 3000 Å,” Appl. Opt. **5,** 937–943 (1966).
68. A. F. Grenis and M. J. Matkovich, “Blackbody reference for temperature above 1200 K. Study for design requirements,” AMRA TR **65,** 1–18 (1965).
69. G. V. Saidov and E. B. Bernstein, “Optical constants of surface layer of fused quartz in the 900–1300 cm^{-1} range,” Fiz. Khim. Stekla **8,** 75–81 (1982).
70. A. M. Efimov, “Dispersion of optical constants of vitreous solids,” Ph.D. dissertation (Vavilov State Optical Institute, Leningrad).
71. R. K. Bogens and A. G. Zhukov, “The optical constants of fused quartz in the far infrared,” J. Appl. Spectrosc. **25,** 54–55 (1966).
72. T. J. Parker, J. E. Ford, and W. G. Chambers, “The optical constants of pure fused quartz in the far-infrared,” Infrared Phys. **18,** 215–219 (1978).
73. A. P. Zhilinskii, A. P. Gorchakov, T. S. Egorova, and N. A. Miskinova, “Optical characteristics of fused quartz in the far IR range,” Opt. Spectrosc. **62,** 783–784 (1987).
74. W. Bagdade and R. Stolen, “Far infrared absorption in fused quartz and soft glass,” J. Phys. Chem. Solids **29,** 2001–2008 (1968).
75. G.-L. Tan, M. F. Lemon, and R. H. French, “Optical properties and London dispersion forces of amorphous silica determined by vacuum ultraviolet spectroscopy and spectroscopic ellipsometry,” J. Am. Ceram. Soc. **86,** 1885–1892 (2003).
76. P. T. T. Wong and E. Whalley, “Infrared and Raman spectra of glasses. Part 2. Far infrared spectrum of vitreous silica in the range 100–15 cm^{-1},” Discuss. Faraday Soc. **50,** 94–102 (1970).
77. R. K. Mamedov, G. M. Mansurov, and N. I. Dubovikov, “Optical constants of quartz glass in the IR range,” Opt. Mekh. Prom. **4,** 56 (1982) [Sov. J. Opt. Technol. **49,** 256 (1982)].
78. M. Miler, “Infrared absorption of glassy silicon dioxide,” Czech. J. Phys. **18,** 354–362 (1968).
79. http://www.tpdsci.com/Tpc/RIQtzFsd.php and http://repositories.cdlib.org/escholarship/.